Sodium chloride methanol solution spin-coating process for bulk-heterojunction polymer solar cells*

Tong-Fang Liu(刘统方)[1], Yu-Feng Hu(胡煜峰)[1,†], Zhen-Bo Deng(邓振波)[1,‡], Xiong Li(李熊)[2], Li-Jie Zhu(朱丽杰)[1], Yue Wang(王越)[1], Long-Feng Lv(吕龙锋)[1], Tie-Ning Wang(王铁宁)[1], Zhi-Dong Lou(娄志东)[1], Yan-Bing Hou(侯延冰)[1], and Feng Teng(滕枫)[1]

[1] *Key Laboratory of Luminescence and Optical Information, Ministry of Education, Beijing Jiaotong University, Beijing* 100044, *China*
[2] *Department of Physics, Beijing Technology and Business University, Beijing* 100048, *China*

(Received 27 January 2016; revised manuscript received 25 February 2016; published online 25 June 2016)

The sodium chloride methanol solution process is conducted on the conventional poly(3-hexylthiophene) (P3HT)/[6,6]-phenyl-C61-butyric acid methyl ester ($PC_{61}BM$) polymer bulk heterojunction solar cells. The device exhibits a power conversion efficiency of up to 3.36%, 18% higher than that of the device without the solution process. The measurements of the active layer by x-ray photoelectron spectroscopy (XPS), atomic force microscopy (AFM), and ultraviolet photoelectron spectroscopy (UPS) indicate a slight phase separation in the vertical direction and a sodium chloride distributed island-like interface between the active layer and the cathode. The capacitance–voltage (C–V) and impedance spectroscopy measurements prove that the sodium chloride methanol process can reduce the electron injection barrier and improve the interfacial contact of polymer solar cells. Therefore, this one-step solution process not only optimizes the phase separation in the active layers but also forms a cathode buffer layer, which can enhance the generation, transport, and collection of photogenerated charge carriers in the device simultaneously. This work indicates that the inexpensive and non-toxic sodium chloride methanol solution process is an efficient one-step method for the low cost manufacturing of polymer solar cells.

Keywords: sodium chloride, methanol, polymer solar cell, phase separation

PACS: 88.40.jr, 84.60.Jt, 64.75.St, 73.50.–h **DOI:** 10.1088/1674-1056/25/8/088801

1. Introduction

Polymer solar cells (PSCs) are promising for low cost roll-to-roll manufacturing of flexible large area photovoltaic devices. To achieve high efficiency devices, the optimized morphology of the active layer for the improved generation and transport of charge carriers and the modified electrode for the facilitated charge extraction are essential.[1–3] The bulk heterojunction (BHJ) is more advantageous in the charge separation than the planar heterojunction due to the improved charge carrier kinetics by forming a morphological idea heterojunction network.[4,5] Thermal/solvent annealing can also enhance the phase separation of the active layer and help the charge separation.[6–8] Some reports indicated that the solvent additive can be used for morphological control in the polymer BHJ solar cells, and thus facilitate the charge separation and transport between the donor and acceptor in the active layer.[9,10] Previous studies have shown that the nanoscale domains of the active layer provide spatially isolated regions in which the holes and electrons can transport.[11] In addition, many groups have found that the device performance could be considerably enhanced by polar solvent treatment, which is thought to optimize the charge separation and transport in PSC active layers.[12–14] On the other hand, the interface engineering is vital to improving the performance of PSCs. Many experiments have reported that the performance of PSCs can be improved by inserting a cathode interfacial layer between the active layer and the cathode.[15] Various interfacial materials, such as metal oxides (e.g., ZnO, TiO_x),[16–19] self-assembled monolayer,[20] lithium fluoride (LiF),[21,22] cesium carbonate (Cs_2CO_3),[23,24] cesium fluoride (CsF),[25] and sodium chloride (NaCl)[26] have been successfully used to enhance the performance of PSCs.

In this study, we demonstrate that the NaCl methanol solution treatment can well improve the device performance of PSCs due to the optimization of the phase separation in the active layer and the formation of a low work function surface in the cathode. The solution process is simpler than the traditional vacuum evaporation. The methanol solution process has some advantages over the deionized water method[26] in polymer solar cells. On one hand, the deionized water is believed to be a bad solvent for most organic materials and favors oxidation or reduction in the device under bias.[27] Especially, it has been reported that the deionized water has a degradation effect on the P3HT:$PC_{61}BM$ solar cells;[28,29] on the other hand, as a solvent, methanol can improve the morphology of the active layer, which is beneficial to the electronic collection and, as a result, improve the performance of

*Project supported by the Fundamental Research Funds for the Central Universities, China (Grant No. 2014JBZ009) and the National Natural Science Foundation of China (Grant Nos. 61274063, 61377028, 61475014, and 61475017).

†Corresponding author. E-mail: yfhu@bjtu.edu.cn
‡Corresponding author. E-mail: zbdeng@bjtu.edu.cn

© 2016 Chinese Physical Society and IOP Publishing Ltd

the solar cells.[12,30,31] Our work demonstrates that the NaCl methanol solution process can help the charge separation and the generation of mobile carriers, transport of photogenerated electrons and holes, as well as the collection of electrons at the cathode. More importantly, this process can be used in the printing electronics manufacturing processes.

2. Experimental details

The device configuration of the PSCs is shown in the inset of Fig. 1(a). Poly(3,4-ethylenedioxythiophene): poly (styrene sulfonate) (PEDOT: PSS; Clevios P Al4083) was purchased from SCM Indus-trial Chemical Co., Ltd. Poly(3-hexylthiophene) (P3HT, Mw = 60000∼80000 g/mol, regioregularity = 95%) was obtained from Rieke Metals Inc., and [6,6]-phenyl-C61-butyric acid methyl ester ($PC_{61}BM$) was purchased from the Nano-C Company. The methanol and NaCl were purchased from Aladdin. For device fabrication, ITO-coated glass substrates were cleaned by ultra-sonication for 30 min in detergent, deionized water, acetone, and eth-anol in sequence, and then dried with N_2. Next ITO-coated glass substrates were treated by ozone-ultraviolet for 15 min. Then the well-cleaned ITO was spin-casted by PEDOT: PSS at 3000 rpm for 50 s, and then dried at 150 °C for 30 min in the air. P3HT and $PC_{61}BM$ were dissolved in chlorobenzene (Alfa Aesar, 95%) to make a 27-mg/ml solution with a weight ratio of 1:0.8, then the blend was stirred for 24 h at 45 °C in the glove box. The active layer was prepared by spin-coating the blend on the PEDOT: PSS layer at 1500 rpm for 50 s, followed with drying at 50 °C for 10 min. The NaCl was dissolved in methanol to make solutions, which were directly spin-coated at the top of the P3HT: $PC_{61}BM$ active layers at 1000 rpm. All of the solution processes were carried out in an air atmosphere. Subsequently, a 100-nm-thick Al layer was evaporated under a pressure of 5×10^{-4} Pa through a shadow mask to determine the active area of the devices (0.045 cm^2).

The devices were tested under one sun, AM 1.5 xenon-lamp-based solar simulator (San-Ei Electric) at 100 mW/cm^2 intensity. Current density–voltage (J–V) characteristics of the devices were measured through a Keithley 6430 Source Measure Unit. The external quantum efficiency (EQE) measurements were carried out by using a solar cell QE/IPCE measurement system (Zolix solar cell scan100). The morphologies of the blend films were investigated by the Shimadzu Corporation SPM-9600 atomic force microscopy (AFM). X-ray photoelectron spectroscopy (XPS) and ultraviolet photoelectron spectroscopy (UPS) were performed using an ESCALAB 250 analysis system. Capacitance–voltage (C–V) measurements and impedance spectroscopy measurements were conducted with an impedance analyzer E4990A Agilent.

3. Results and discussion

The device performances are exhibited in Fig. 1 and the results are summarized in Table 1. The device with the NaCl methanol solution treatment shows a significant improvement of PCE up to 3.36%, while the PCEs of the devices with the methanol treatment and without treatment are 3.13% and 2.84%, respectively. The increasing trends of J_{sc} and FF from the device with the methanol treatment agree well with previous results.[12,30,31] The EQE exhibits a maximum value of 61% near 470 nm and the EQE enhancement is in a wavelength range from 350 nm to 600 nm with the NaCl methanol solution process, which is in good agreement with the J–V characteristics.

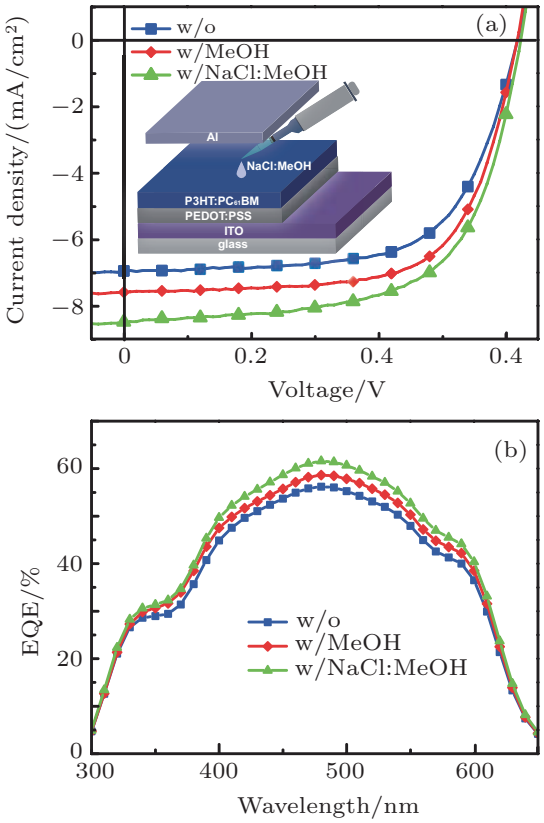


Fig. 1. (color online) (a) J–V curves for P3HT:$PC_{61}BM$-based PSCs with or without (w/o) treatment under an illumination of 100 mW/cm^2, and the inset shows the configuration of the PSCs. (b) EQEs of the PSCs with or without treatment.

Table 1. Photovoltaic parameters of the PSCs with or without treatment based on over twenty devices.

Device	J_{SC}/(mA/cm^2)	V_{OC}/V	FF/%	PCE/%
w/o	7.0 ± 0.1	0.62 ± 0.01	64.9 ± 0.5	2.84 ± 0.06
w/MeOH	7.4 ± 0.1	0.62 ± 0.01	67.5 ± 0.4	3.13 ± 0.04
w/NaCl:MeOH	8.5 ± 0.2	0.62 ± 0.01	63.8 ± 0.9	3.36 ± 0.08

The surface morphologies of the P3HT:$PC_{61}BM$ films are imaged by AFM, and the images of the control devices (without treatment and with the methanol treatment) and the NaCl methanol solution processed device are shown in Fig. 2. It implies that the methanol treatment causes a little change in morphology, and the film surface roughness has a slight increase, from 0.99 nm to 1.15 nm while the surface roughness of the NaCl methanol solution processed device is up to 2.49 nm, forming an island-like distributed layer.

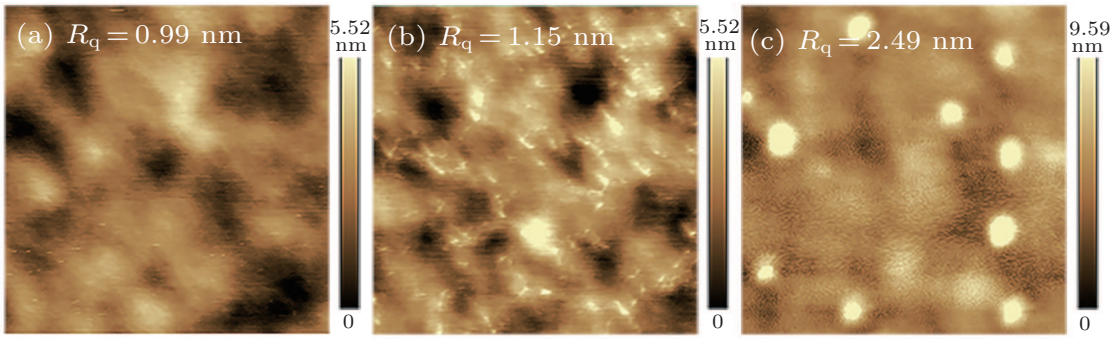


Fig. 2. (color online) AFM (1 μm×1 μm) images of P3HT:$PC_{61}BM$ blend films without treatment (a), with methanol (b), with methanol-processed NaCl (c). The root mean square roughness (R_q) is marked in each image.

The surface compositions of the films are tested by XPS, and the results are shown in Table 2. It is known that carbon atoms exist in both P3HT and $PC_{61}BM$, while sulfur and sodium only exist in P3HT and NaCl respectively. Therefore, the C (1s) peak represents the total content of P3HT and $PC_{61}BM$, S (2p) peak represents the content of P3HT, and the S (2p)/C (1s) peak area ratio could be proportional to the percentage of P3HT in the composite. Similarly, the Na (1s) peak represents the content of NaCl.

Table 2. Atomic fractions at the top surfaces of P3HT:$PC_{61}BM$ blend films with or without treatment.

Device	Atomic/%			
	C (1s)	S (2p)	Na (1s)	S (2p)/ C (1s)
w/o	98.77	1.23	–	1.23/98.77
w/MeOH	99.14	0.86	–	0.86/99.14
w/NaCl:MeOH	98.71	1.15	0.14	1.15/98.85

The atomic fractions of C (1s), S (2p), Na (1s), and S (2p)/C (1s) atomic ratios at the top surfaces of the various films show that the S (2p) atomic fraction declines from 1.23% to 0.86% after the methanol treatment, indicating that $PC_{61}BM$ diffuses to the top surface. The methanol treatment can improve the distribution of the active layer and slightly enhance the vertical phase separation. Then, after the NaCl methanol solution treatment, the decline of S (2p) atom occurs, while the Na (1s) atom signal can also be detected with an atomic fraction of 0.14%. The P3HT:$PC_{61}BM$ weight ratios at the bottom and top surfaces can be evaluated by using S (2p)/C (1s) atomic ratios. The S (2p)/C (1s) atomic ratios for the devices with the methanol or NaCl methanol solution treatments are lower than the one without treatment. It should be pointed out that the device with methanol treatment has a little lower S (2p)/C (1s) atomic ratio than the device with NaCl methanol solution process, and it is possible that the NaCl crystal has a slight blocking effect. Anyway, these results imply that the methanol treatment is conductive to the vertical phase separation. And the crystal in Fig. 2 is NaCl.

The various Al surface properties are investigated by ultraviolet photoelectron spectroscopy (UPS). The 50-nm-thick Al films are deposited on the ITO substrates and then modified with the methanol and NaCl methanol solution processes. Figure 3(a) shows the UPS spectra of the Al with and without solution treatment. There is a little shift of the electron cut-off energy towards higher binding energies after the NaCl methanol solution process. The energy level alignment of each component of the PSCs based on P3HT:$PC_{61}BM$ is shown in Fig. 3(b). The work function of the Al surface is lowered by 0.14 eV with the NaCl methanol solution treatment while the binding energy of Al surface with the methanol treatment has no obvious change compared with the device without solution treatment. Therefore, the decrease of the work function is mainly due to the insertion of a NaCl layer, which reduces the electron collection barrier and therefore enhances the collection of mobile carriers.

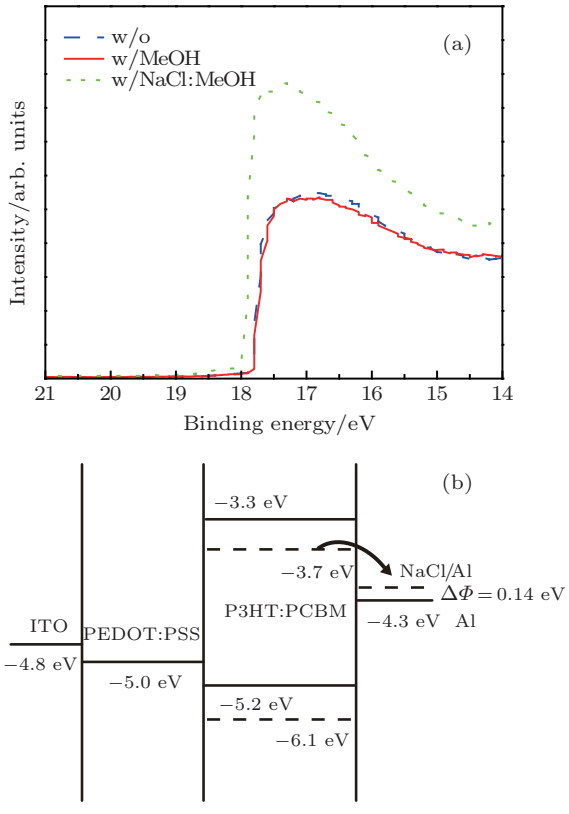


Fig. 3. (color online) (a) UPS spectra of Al surface with and without treatment. (b) The band alignment of the component of the PSCs based on P3HT:$PC_{61}BM$.

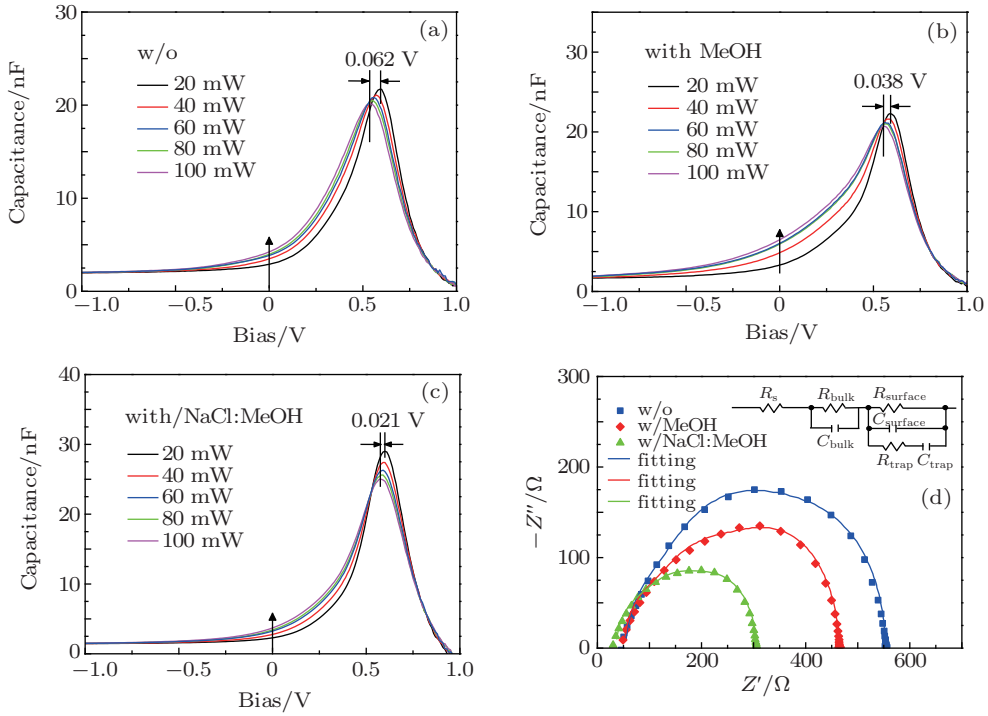


Fig. 4. (color online) *C–V* characteristics under different photoexcitation intensities and impedance spectra of the PSCs based on P3HT:$PC_{61}BM$. (a) *C–V* characteristics of the device without treatment. (b) *C–V* characteristics of the device with methanol treatment. (c) *C–V* characteristics of the device with NaCl methanol treatment. (d) Impedance spectra with or without treatment.

The *C–V* characteristics of the different devices shown in Figs. 4(a)–4(c) are obtained at the various photo-excitation intensities between 20 mW/cm^2 and 100 mW/cm^2. The particular *C–V* characteristic is used to directly explore the effects of the dielectric interface on the surface accumulation and collection. The carriers accumulate at the inter-face before the peak and begin to be injected into the active layer from the interface at the peak.[32,33] Therefore, the V_{peak} is the critical voltage required to initiate the charge injection from the electrode into the active film in PSCs, which reflects the effective interfacial barrier. When the bias is constant, with the increase of the light intensity, the capacitance basically shows an increasing trend, which can be explained by the fact that photo-generated carriers lead to the increase of the total charge quantity at the interface. When the light intensity is increased, the V_{peak} in the *C–V* characteristic shifts to a lower value. The reason why the V_{peak} shifts can be discussed as follows. Under the photoexcitation, the charge carriers at the active layer/electrode interfaces lower the potential barrier. Therefore, the V_{peak} shifts to a lower value with increasing the light intensity, which can reveal the accumulation of photogenerated carriers at the active layer/electrode interface. In other words, the photo-generated charges accumulated at the interface lead to a reduced V_{peak} value. The observed V_{peak} shifts are 0.062 V and 0.038 V for the devices without treatment and with the methanol treatment respectively, while the device with the NaCl methanol solution process exhibits a much smaller V_{peak} shift of 0.021 V. Therefore, the comparison of the V_{peak} shifts indicates that the solar cell with the NaCl methanol solution treatment has a lesser accumulation of the photo-generated charges at the interface.

The impedance spectrum is measured at a direct current (DC) forward bias of 0.62 V under dark conditions. Figure 4(d) shows that the Nyquist plots of the impedance measurement of the P3HT:$PC_{61}BM$ devices with methanol treatment, with NaCl methanol solution treatment, and without any treatment for the frequencies from 20 Hz to 2 MHz respectively. These plots are the complex plane representations of the imaginary part of the impedance response (reactance or Z'') and the real part of the impedance (resistance or Z'). The devices each exhibit a single semicircle in the complex plane whose diameter represents a negative capacitance and its origin is attributed to the surface traps or the interfacial barriers.[34,35] While the active layer conditions are the same, the different diameters (resistance) clearly correspond to the differences in contact resistance among these three devices. It is interesting that there is a significant difference in impedance spectrum among these three devices. The device without treatment shows the largest diameter and the methanol treated device takes the second place, moreover, the NaCl methanol solution treated device has the smallest diameter. The series resistance (R_s) can be obtained from the fitting data by using the equivalent circuit modelling. The series resistances are 2.50 Ω·cm^2 and 2.33 Ω·cm^2 for the devices without any treatment and with the methanol treatment, respectively, while the R_s is 1.76 Ω·cm^2 with the NaCl methanol process. Most likely the NaCl methanol solution process both improves the active layer phase separation and forms a more efficient cathode contact. Therefore, the impedance spectra have exactly the same trend as those derived from *J–V* data and *C–V* characteristics for the devices with or without the treatments.

4. Conclusions

We investigate the effect of the sodium chloride methanol process for bulk heterojunction organic solar cells. The XPS analysis of the active layer reveals a slight phase separation in the vertical direction and sodium chloride distributed island-like interface between the active layer and the cathode on the top surface. The *C–V* and impedance spectrum measurements prove that the sodium chloride methanol process can reduce the electron injection barrier and improve the interfacial contact of polymer solar cells. This work demonstrates that the sodium chloride methanol solution treatment can facilitate photoinduced charge separation, the generation of mobile carriers, and the collection of electrons.

Acknowledgment

We are grateful to Dr. Ye Zou for XPS and UPS test.

References

[1] Li G, Zhu R and Yang Y 2012 *Nat. Photon.* **6** 153
[2] Dou L, You J, Hong Z, Xu Z, Li G, Street R A and Yang Y 2013 *Adv. Mater.* **25** 6642
[3] Heeger A J 2014 *Adv. Mater.* **26** 10
[4] Yang F, Shtein M and Forrest S R 2005 *Nat. Mater.* **4** 37
[5] Blom P W M, Mihailetchi V D, Koster L J A and Markov D E 2007 *Adv. Mater.* **19** 1551
[6] Ma W, Yang C, Gong X, Lee K and Heeger A J 2005 *Adv. Funct. Mater.* **15** 1617
[7] Fan X, Zhao S L, Chen Y, Zhang J, Yang Q, Gong W, Xu Z and Xu X 2015 *Chin. Phys. Lett.* **32** 161
[8] Li G, Shrotriya V, Huang J, Yao Y, Moriarty T, Emery K and Yang Y 2005 *Nat. Mater.* **4** 864
[9] Xiao Z, Yuan Y, Yang B, VanDerslice J, Chen J, Dyck O, Duscher G and Huang J 2014 *Adv. Mater.* **26** 3068
[10] Yan S, Lv L, Ning Y, Qin L, Li C, Liu X, Hu Y, Lou Z, Teng F and Hou Y 2015 *Phys. Status Solidi A* **212** 2169
[11] Laquai F, Andrienko D, Mauer R and Blom P W M 2015 *Macromol. Rapid Comm.* **36** 1001
[12] Zhou H, Zhang Y, Seifter J, Collins S D, Luo C, Bazan G C, Nguyen T and Heeger A J 2013 *Adv. Mater.* **25** 1646
[13] Li H, Tang H, Li L, Xu W, Zhao X and Yang X 2011 *J. Mater. Chem.* **21** 6563
[14] Liu Y, Lv L, Ning Y, Lu Y, Lu Q, Zhang C, Fang Y, Tang A, Hu Y, Lou Z, Teng F and Hou Y 2014 *Chin. Phys. B* **23** 118802
[15] Chen F, Chen Q, Mao L, Wang Y, Huang X, Lu W, Wang B and Chen L 2013 *Nanotechnology* **24** 484011
[16] Small C E, Chen S, Subbiah J, Amb C M, Tsang S, Lai T, Reynolds J R and So F 2012 *Nat. Photon.* **6** 115
[17] Sun Y, Seo J H, Takacs C J, Seifter J and Heeger A J 2011 *Adv. Mater.* **23** 1679
[18] Choi H, Park J S, Jeong E, Kim G H, Lee B R, Kim S O, Song M H, Woo H Y and Kim J Y 2011 *Adv. Mater.* **23** 2759
[19] Lv L, Lu Q, Ning Y, Lu Z, Wang X, Lou Z, Tang A, Hu Y, Teng F, Yin Y and Hou Y 2015 *Chem. Mater.* **27** 44
[20] De Boer B, Hadipour A, Mandoc M M, van Woudenbergh T and Blom P W 2005 *Adv. Mater.* **17** 621
[21] Brabec C J, Shaheen S E, Winder C, Sariciftci N S and Denk P 2002 *Appl. Phys. Lett.* **80** 1288
[22] Padinger F, Rittberger R S and Sariciftci N S 2003 *Adv. Funct. Mater.* **13** 85
[23] Huang J, Xu Z and Yang Y 2007 *Adv. Funct. Mater.* **17** 1966
[24] Li G, Chu C W, Shrotriya V, Huang J and Yang Y 2006 *Appl. Phys. Lett.* **88** 253503
[25] Reinhard M, Hanisch J, Zhang Z, Ahlswede E, Colsmann A and Lemmer U 2011 *Appl. Phys. Lett.* **98** 53303
[26] Nickel F, Reinhard M, Zhang Z, Pütz A, Kettlitz S, Lemmer U and Colsmann A 2012 *Appl. Phys. Lett.* **101** 53309
[27] Yahiro M, Zou D and Tsutsui T 2000 *Synthetic Met.* **111** 245
[28] Norrman K, Ma dsen M V, Gevorgyan S A and Krebs F C 2010 *J. Am. Chem. Soc.* **132** 16883
[29] Shambayati S 2011 "Degradation of P3HT: PCBM-based Conjugated Polymer Solar Cells", MS Dissertation (Vancouver: University of British Columbia)
[30] Zang H, Hsiao Y and Hu B 2014 *Phys. Chem. Chem. Phys.* **16** 4971
[31] Zhang K, Hu Z, Duan C, Ying L, Huang F and Cao Y 2013 *Nanotechnology* **24** 484003
[32] Hsiao Y, Zang H, Ivanov I, Xu T, Lu L, Yu L and Hu B 2014 *J. Appl. Phys.* **115** 154506
[33] Seo J H, Gutacker A, Sun Y, Wu H, Huang F, Cao Y, Scherf U, Heeger A J and Bazan G C 2011 *J. Am. Chem. Soc.* **133** 8416
[34] Leever B J, Bailey C A, Marks T J, Hersam M C and Durstock M F 2012 *Adv. Energy Mater.* **2** 120
[35] You J, Chen C, Dou L, Murase S, Duan H, Hawks S A, Xu T, Son H J, Yu L, Li G and Yang Y 2012 *Adv. Mater.* **24** 5267